Three-Dimensional Quantitative Structure−Activity Relationship (QSAR) and Receptor Mapping of Cytochrome P-450$_{14\alpha DM}$ Inhibiting Azole Antifungal Agents[1]

Tanaji T. Talele and Vithal M. Kulkarni*

Pharmaceutical Division, Department of Chemical Technology, University of Mumbai, Mumbai 400 019, India

Received April 13, 1998

Molecular modeling was performed by a combined use of conformational analysis and 3D-QSAR methods to distinguish structural attributes common to a series of azole antifungal agents. Apex-3D program was used to recognize the common biophoric structural patterns of 13 diverse sets of azole antifungal compounds demonstrating different magnitudes of biological activity. Apex-3D identified three common biophoric features significant for activity: N1 atom of azole ring, the aromatic ring centroid 1, and aromatic ring centroid 2. A common biophore model proposed from the Apex-3D analysis can be useful for the design of novel cytochrome P-450$_{14\alpha DM}$ inhibiting antifungal agents.

INTRODUCTION

Cytochrome P-450 dependent lanosterol 14α-demethylase (P-450$_{DM}$) catalyzes the transformation of lanosterol to ergosterol, an important constituent of the cell membrane in fungi by causing the elimination of 14α methyl group of lanosterol to give the C14−C15 unsaturated sterol.[2,3] The accumulation of 14α-methylated sterols in azole-treated fungal cells affects membrane structure and functions, resulting in an inhibition of the growth of fungi. Differential inhibition of this enzyme between pathogenic fungi and man is the basis for the clinically important activity of these azole antifungal agents. The specificity of the inhibitors is determined by the differential complementarity between the structure of the agent and the active sites of the fungal and host enzymes.[4] In fact, one of the reasons to perceive the search for superior antifungal agents is to increase their specificity toward fungal enzyme. This is a crucial purpose especially under pathological cases where the immune system is compromised to a great extent (AIDS pathology) and the side effects (inhibition of the host P-450) due to overdosage of the azole compounds may eventually cause the death of patients.[5,6]

In an effort to illustrate azole binding sites and to develop common structural features among azole antifungal agents, the structure−activity relationship (SAR) of various azole class inhibitors have been studied. On the basis of SAR studies, the structural similarities between azole antifungal agents that directly contribute to binding and selectivity for cytochrome P-450$_{14\alpha DM}$ receptor have been identified.

Since no structural information is available about the azole antifungal compounds in complex with cytochrome P-450$_{14\alpha DM}$ enzyme, an indirect approach was implemented in an attempt to understand the important interactions necessary for binding. This approach is referred to as receptor mapping or biophore (pharmacophore) identification. In the present work, we describe a three-dimensional quantitative structure−activity relationship (3D-QSAR) using Apex-3D (Molecular Simulations Inc.) program, of 13 azole antifungal compounds found to active in vitro against *C. albicans*. The compounds that have been studied as shown in Figure 1.[7−15] These compounds are characterized by sterically accessible conformational analysis, to search for a common relative spatial disposition of molecular features appropriate for biological activity. A statistically significant common spatial biophore identified by Apex-3D has been proposed for these ligands. The atoms considered in the biophore definition in each compound are labeled in Figure 1, and their main interatomic distances between the biophoric descriptors are shown in Figure 2. A 3D-QSAR method[16,17] was used to build a valid 3D geometrical model for azole antifungal agents. The geometrical requirements for each compound are described by using interatomic distances between the three descriptors that are present in all the training sets of compounds which were considered most significant for interaction with cytochrome P-450$_{14\alpha DM}$ receptor. Steric and electronic properties were calculated and used in the evaluation of similarity between the compounds upon identification of active conformations of each ligand.

COMPUTATIONAL METHODS

The molecular structures of azole antifungals were drawn in 2D and converted to 3D using the *Sketch* and *Converter* module in INSIGHT 95.0[18] and then energy minimized (using steepest descent and conjugate gradient algorithms) to afford a reasonable standard geometry.

A systematic conformational search in the *Search*/*Compare* module identified the sterically accessible conformations for these structures using a rotation increment of 15° for all the torsional angles. These conformational results were confirmed by means of the molecular mechanics method using the conjugate gradient algorithm of the Discover 3.0 program (Molecular Simulations Inc.).[19] The list of allowed conformations was too large; therefore the lowest energy conformers for each compound having potential energies below 10 kcal mol^{-1} of the current global minimum were saved.[20]

Further Apex-3D was used for automated pharmacophore identification and 3D-QSAR model building. Statistically significant biophores and their active conformations from Apex-3D analysis were used in the calculation of molecular

10.1021/ci9800413 CCC: $18.00
Published on Web 01/13/1999

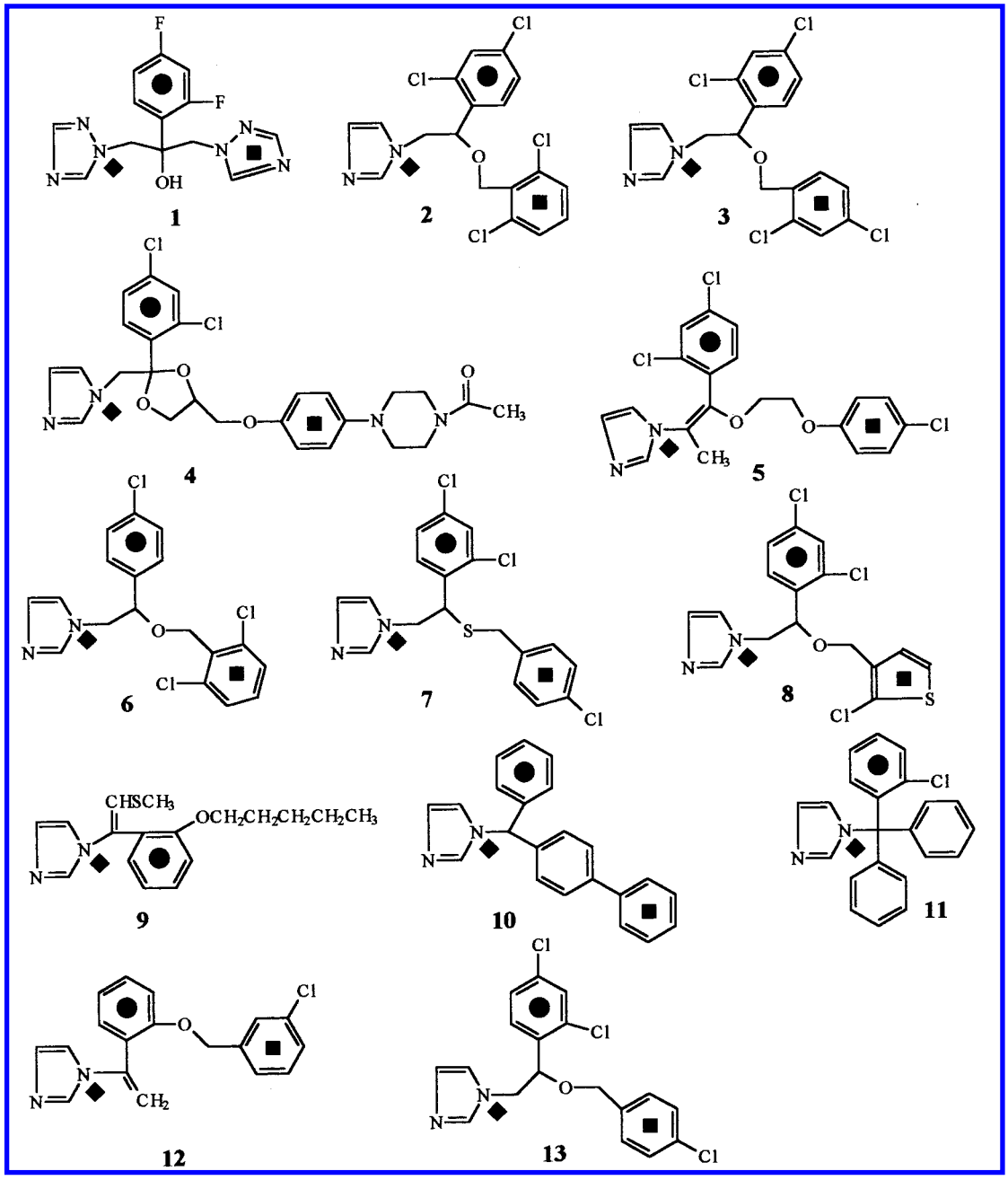

Figure 1. Structures of 13 training set of azole antifungal compounds. The atoms labeled ◆, ●, ■ are the main structural features (biophores) identified by Apex-3D.

volumes. Volumes were visualized through Boolean grid representations of the superimposed molecules generated using the *volume*/*create* option of INSIGHT 95.0.

The electrostatic potential similarities[21] between each pair of molecules as well as the overall similarity were calculated, and the potential similarities were analyzed by optimizing the fit. All the calculations were performed on a Silicon Graphics Indigo^2 Solid Impact R4400 workstation.

RESULTS AND DISCUSSION

The aim of the present work has been the development of a common pharmacophore model for the diverse set of compounds that have the binding affinity for the cytochrome P-450$_{14\alpha DM}$ receptor. From conformational analysis, the lowest energy conformer of each compound was considered as the active conformer and compared with the low-energy conformers of all the other compounds to achieve a common alignment (optimization of superimposition) model which accommodates all the compounds. The Apex-3D program was used for the automated pharmacophore identification and 3D-QSAR model building to construct an active model for the cytochrome P-450$_{14\alpha DM}$ receptor. The approach should thus be useful for the design of new cytochrome P-450$_{14\alpha DM}$ inhibiting antifungal agents.

Conformational Analysis. To identify statistically significant biophore for these flexible compounds, a set of conformers was generated by a systematic conformational search method using molecular mechanics CVFF (consistent valence force field) calculations as described in the computational methods section. The low-energy bioactive conformers were identified that represent the pharmacophore. Due to the high flexibility of these compounds, the number of

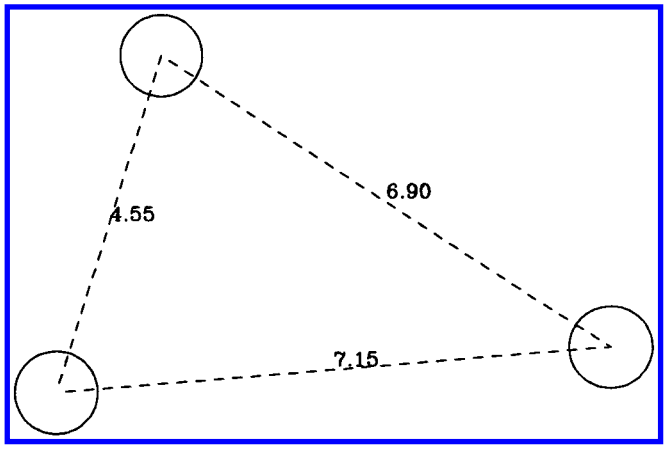

Figure 2. View of the biophore and the important descriptors considered in the biophore definition. The distance ranges are given in Å.

Table 1. Conformational Energy Data and Biological Activity of Cytochrome P-450$_{14\alpha DM}$ Inhibiting Azole Compounds

compd	conformers[a]	energy[b] (*E*)	MIC[c]
1	38	8.28	−0.53
2	12	3.63	2.00
3	49	3.07	1.00
4	52	4.81	−2.00
5	55	4.08	−0.43
6	7	2.65	1.00
7	30	3.73	0.71
8	57	2.21	1.10
9	15	1.87	0.81
10	7	2.90	0.40
11	3	8.55	0.87
12	46	2.62	1.80
13	13	3.49	2.00

[a] Within 10 kcal mol^{-1} above that of the lowest energy conformation found. [b] Energy difference between the Apex-3D conformer and the lowest energy conformer. [c] Biological activity (MIC in μg/mL) is expressed as (log MIC).

conformers generated were too large, a *set_energy_params* command was used to control the maximum conformers up to 100 and the molecular mechanics energy threshold to 10 kcal mol^{-1} to reduce the number of conformers that are energetically most stable. This process effectively excluded those conformers that were not unique. To filter out conformers that will not add new information on biophore geometry and resultant superimpositioning of these flexible ligands, Apex-3D was then used for internal conformer clusterization in which the sample of conformers for each compound is partitioned into a number of clusters.[22] After the conformer clustering, the lowest energy conformer of each cluster is selected as representative of that cluster and exported to Apex-3D, which is available in INSIGHT II (95.0) software for automated biophore identification and 3D-QSAR model building. Having determined the lowest energy state of each of the compounds, the energy of each compound when it was in the pharmacophoric configuration was calculated and compared to determine whether the pharmacophoric conformation was a viable entity or a modeling artifact and shown in Table 1. The best fit for pharmacophoric conformers of all the 11 compounds of Model I are shown superimposed in Figure 3. All the data set compounds except compounds **1** and **11** were able to attain a common pharmacophoric configuration with a moderate energy penalty (<5 kcal) that represents the difference in energy of the pharmacophoric and the lowest energy conformations. In a biological milieu (e.g. receptor binding site) this penalty should be easily accommodated because of favorable interactions with the receptor. Inherent in the comparison of the pharmacophoric conformation versus the energetically most favorable conformation is the concept that the biologically active conformation of a molecule need not be the one of the lowest energy. As mentioned above, this concept looks reasonable because attention must be given for conformers within energetic reach of perturbations due to receptor interactions. Hence, determination of absolute low-energy conformations become less important in describing the pharmacophore geometry.[23]

Apex-3D Analysis. Apex-3D uses a logico-structural approach[24] to identify molecular features common to a set of diverse chemical structures. Advanced statistical techniques and 3D pattern-matching algorithms are used to assign

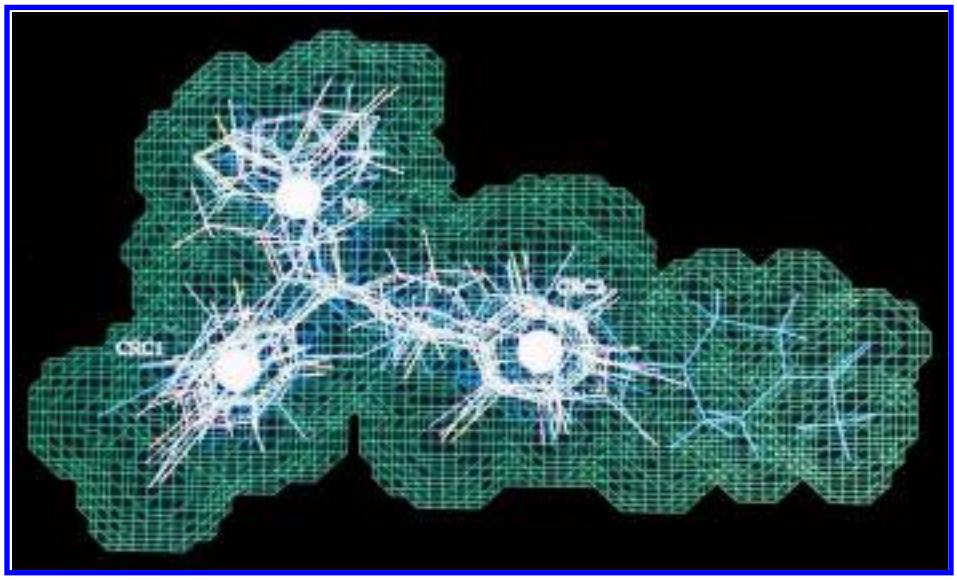

Figure 3. "Pharmacophore" conformations of the **11** compounds and the excluded volume map of cytochrome P-450$_{14\alpha DM}$ receptor. Note overlap of pharmacophoric atoms (N1, CRC1, and CRC2). The volume shown as green wire mesh is defined by a union of **11** compounds van der Waals density maps and represents the volume that is available for drugs interacting with ctyochrome P-450$_{14\alpha DM}$ receptor.

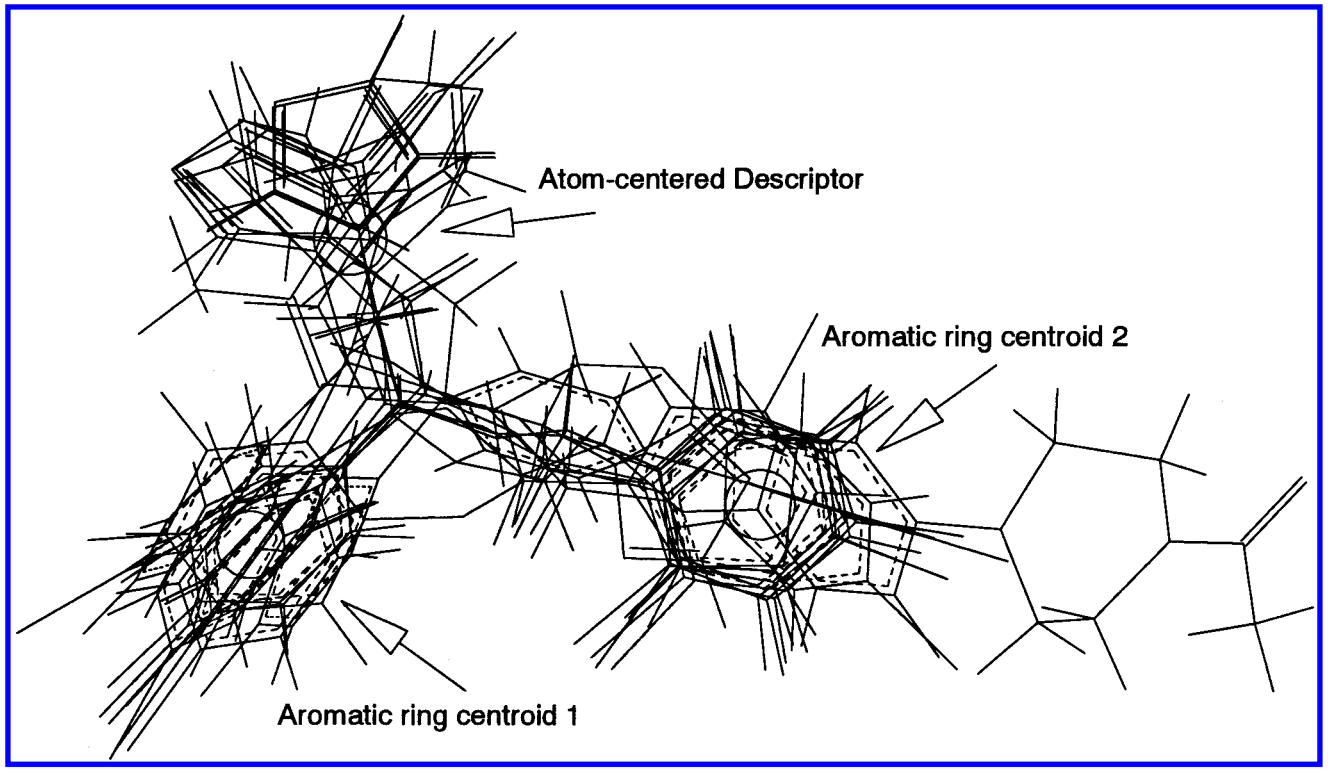

Figure 4. Optimization of superimposition (alignment) and biophoric site points of a statistically significant biophore model I identified by Apex-3D. White spheres denote one atom-centered descriptor and two ring centers.

Table 2. APEX-3D Model Reliability Evaluation

no. of compds	model	RMSA	RMSP	R^2	chance	match
11	I	0.38	0.37	0.93	0.06	0.64
13	II	0.32	0.35	0.94	0.09	0.57
11	III	0.42	0.46	0.93	0.08	0.61
11	IV	0.51	0.63	0.90	0.09	0.61
12	V	0.54	0.62	0.84	0.07	0.61

probabilities for the identified biophores that are contributing to the biological activity of these compounds. These biophores are composed of various descriptor centers. Calculations with Apex-3D were performed on these sets of compounds. Apex-3D was asked to consider the following properties for structure−activity relationships: charge, ACC_01, hydrophobicity, steric, aromatic ring centroids. One of the statistically significant alignment model is identified, and its pharmacophore site points are shown in Figure 4. Apex-3D identified the following features important for activity that included all the training compounds (Table 1) superimposed onto three distinct pharmacophoric site points: one atom centered descriptor and two aromatic ring centers. Initially, five models were selected with one model associated with each conformer of the training set. The selection of an appropriate model is based on the minimal deviation of the superimposed biophoric centers, the best possible fit of each of the superimposed ensembles, and the results obtained from 3D-QSAR analysis. A pharmacologically relevant model would be associated with an initial positive R^2 when considered in the training set. This hypothesis was used as an initial screening process whereby each model was subjected for 3D-QSAR reliability checking. The results of initial analysis are listed in Table 2. During the selection of significant biophore model, compounds having a large difference in leave-one-out predictions the RMSA (root-mean-square error of activity approximation)

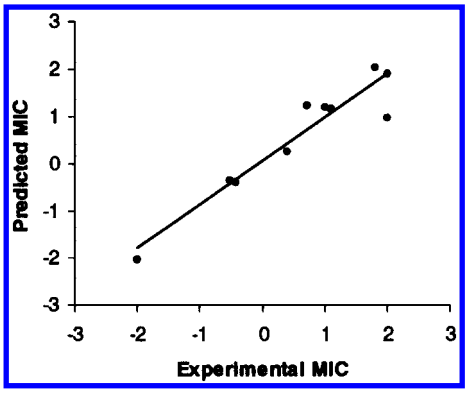

Figure 5. Plot of experimental versus predicted MIC values for the set of 11 cytochrome P-450$_{14\alpha DM}$ inhibiting azole antifungal agents belonging to model I.

and RMSP (root-mean-square error of activity prediction calculated using cross validation) that are over fitted by the multiple regression and are poorly predicted were not included in the training set. The probability of chance correlations greater than 0.1 were not considered further. Biophores that have representative compounds with a high match were subsequently used in 3D-QSAR model building. The statistically most significant model I having 11 compounds in the training set was considered. None of the structural features of these compounds (except compound **9** and **11**) extended beyond the steric region, whereas compounds **9** and **11** are not aligned in this model were eliminated. Compound **9** is excluded from model I: the reason is that this particular compound possesses only one aromatic ring center instead of two. Volume difference map between the compounds **1**−**8**, **10**−**13** and compound **9** is shown in Figure 6. Even though compound **11** possesses the pharmacophoric atoms, some parts of its pharmacophore conformation is oriented outside the excluded volume map.

This was further explained by calculating the volume difference between the compounds **1**−**10**, **12**, **13** and compound **11** as shown in Figure 7. This demonstrates that compound **11** protrudes from the receptor excluded-volume, though this compound is active. The reason may be that these protruded portions of this compound must be binding in an extended pocket in the receptor. A superimposition of compound **11** with the other 12 compounds within the ligand-excluded space illustrates that the binding region would require specific volume or may have an auxiliary binding region that can accommodate large substituents such as those associated with compound **11**. This additional volume of this compound apparently is filled by the receptor and unapproachable for ligand binding; this volume is termed as the receptor essential volume.[25] Electrostatic potential similarity calculations were performed and are discussed in the Volumes section.

3D QSAR. The basic statistical tool for 3D-QSAR model building in Apex-3D is the stepwise regression algorithm.[16] This algorithm selects multiple regression equations by deleting and adding variables using F-test criteria. The regression analysis was performed on the training set of compounds of five models obtained from initial model building. The results of statistically significant biophore models of regression analysis applied on the training set data are reported in Table 2. The stepwise F-test performed on the PRESS (prediction sum of squares) values with no cross-validation justifies model I as the most appropriate pharmacophore alignment. The accuracy of the non-cross-validated predictions was assessed by observing the resulting prediction error values. The results of 3D-QSAR studies are presented in Table 3. The difference between the observed and predicted MIC (MIC μg/mL expressed as log MIC for azole antifungal agents against *Candida* spp.) values are listed in

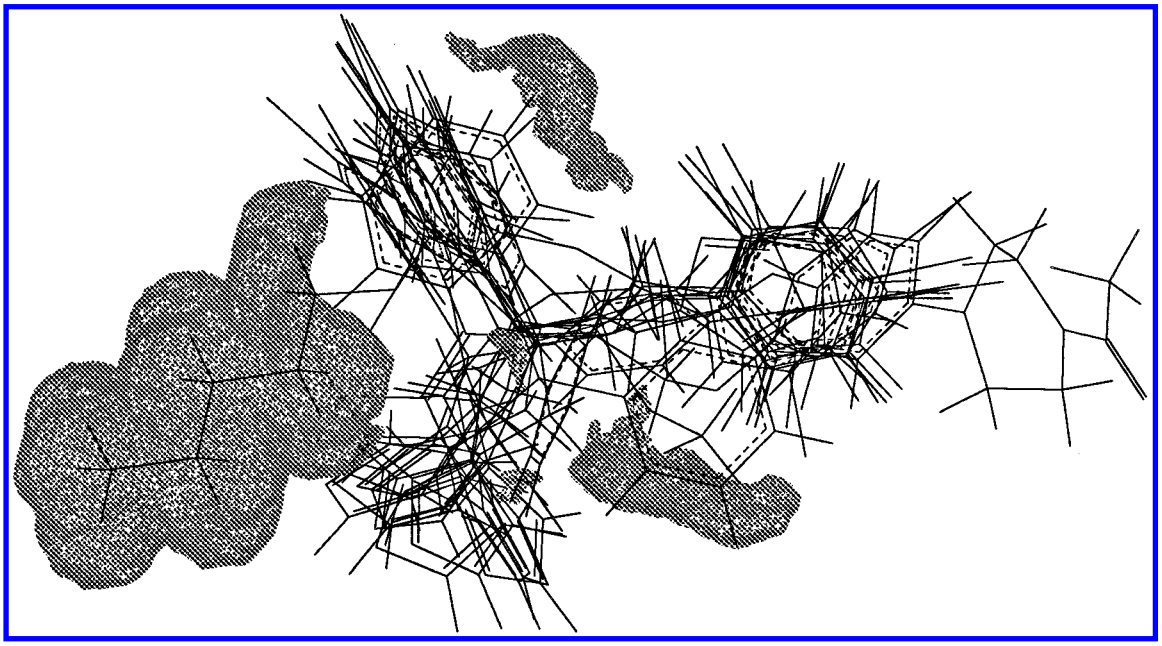

Figure 6. The volume difference of compound **9** with **1**−**8** and **10**−**13**. The most significant difference is occupied by pentoxy group.

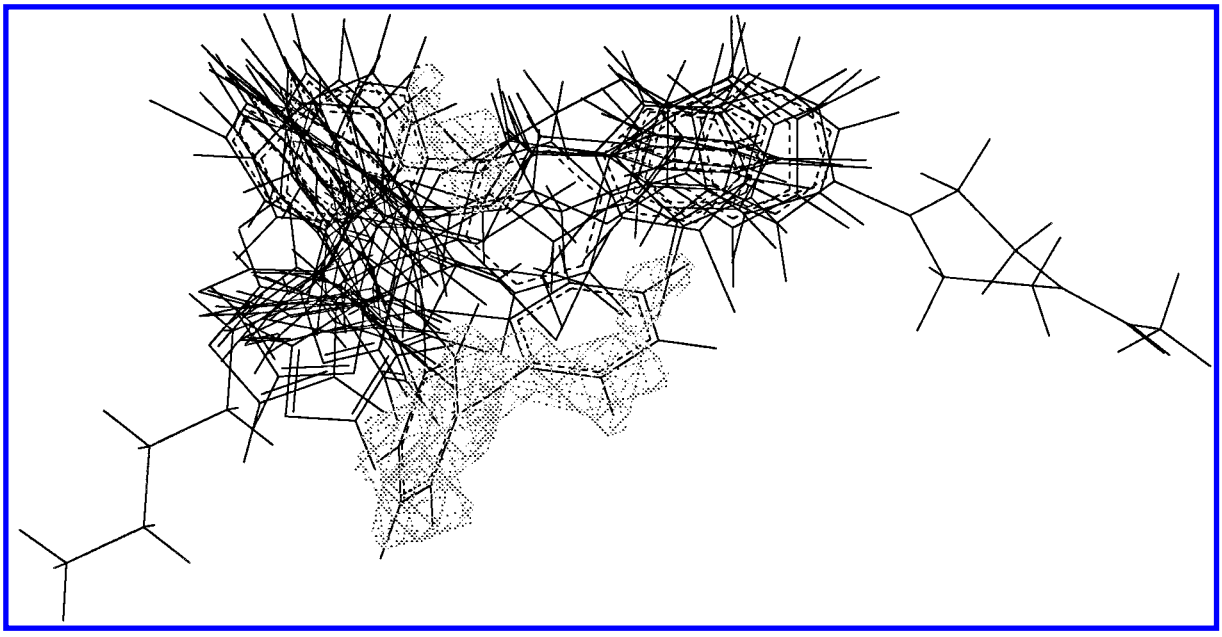

Figure 7. The volume difference of compound **11** with **1**−**10** and **12**, **13**. The most significant difference is occupied by two phenyl rings.

Table 3. APEX-3D Statistical Parameters for MIC Data of Azole Antifungal Agents

	3D-QSAR models				
	I	II	III	IV	V
r^2 non-cross[a]	0.934	0.945	0.931	0.897	0.844
PRESS[b]	1.546	1.617	2.353	4.320	4.649
S[c]	0.377	0.324	0.416	0.507	0.543
F-test	32.924	34.080	20.300	13.121	14.388
n[d]	11	13	11	11	12
contributions[e]					
total_hydrophobicity		1.426	2.322	3.75	
steric (site 1)	1.56	0.74	0.77	1.48	2.27
steric (site 2)	1.60	−0.53	3.15	2.81	1.34
steric (site 3)	−0.78		−1.83	0.97	0.97
hydrophobic (site 4)		1.21			

[a] r^2 represents the non-cross-validated square of the correlation coefficient between experimental and approximated activity. [b] PRESS represents the prediction sum of squares for residuals. [c] S represents RMSA (root-mean-square error of activity approximation). [d] n represents the number of compounds in the training set. [e] Average model variable contributions.

Table 4. Structure−Activity Data of the Experimental and Predicted MICs from APEX-3D Analysis

	3D-QSAR models					
compd	I	II	III	IV	V	exptl
1	−0.37	−0.61	−0.14	0.40	0.76	−0.53
2	1.89	2.50	1.64	1.73	1.65	2.00
3	1.18	0.68	2.07	2.05	1.94	1.00
4	−2.04	−1.76	−1.85	−1.44	−1.70	−2.00
5	−0.39	−0.20	−0.38	−0.60	−0.73	−0.43
6	1.18	1.35	0.52	1.45	0.63	1.00
7	1.24	0.55	1.13	0.88	0.26	0.71
8	1.16	1.00	1.03	0.53	0.10	1.10
9		0.79				0.81
10	0.25	0.81	0.25	−0.17	0.93	0.40
11		0.78			0.70	0.87
12	2.02	1.88	1.94	1.59	1.71	1.80
13	0.96	1.13	1.33	1.22	1.65	2.00

Table 4 and plotted in Figure 5. To visualize the information contents of the 3D-QSAR model, biophore pseudoatoms were generated, and a reliable model for 3D-QSAR coefficients and their associated standard deviations were calculated. Initial analysis based on model I provided a correlation with a non-cross-validated r^2 of 0.934 (F = 32.924) using 11 training set compounds. The RMSA is 0.38 and RMSP is 0.37, which demonstrates a good predictive ability (the coefficient of correlation is 0.966) for the training set of azole antifungals with an average mean-square variance of 0.142. We found that steric sites (site1, site2, and site3) are contributing significantly for the antifungal activity of these compounds. PRESS value and standard deviation of model I is the lowest along with higher F value (32.924) and non-cross-validated r^2 (0.934), thus should be the most robust model with high predictive potential. The following equation shows significant correlation of the efficacy of these compounds as antifungals:

$$\text{activity} = -1.230\ \text{MIC} + 1.563\ (\text{steric site 1}) + 1.597\ (\text{steric site 2}) - 0.785\ (\text{steric site 3})$$

$$n = 11, \quad r^2 = 0.93, \quad \text{RMSA} = 0.38, \quad \text{RMSP} = 0.37$$

Thus steric properties are good descriptors of the activity of these compounds.

Model II yielded a good correlation (r^2 = 0.945 with 13 compounds) and prediction RMSE (0.352), chance correlation was higher (0.09), and match was poor compare to model I. There was no improvement by changing sensitivity and variables. The RMSA was 0.32 and the prediction error was 0.353. The conventional statistical results and the predictive ability of this model for 13 training set compounds were not affected by the changes in the secondary sites. Model III produced a statistically significant correlation (0.931) with average analysis variance of 0.173. The probability of chance correlation and PRESS values are higher 0.08 and 2.353, respectively, along with low F value (20.300). Hence, robustness of this model is lesser than model I and II and not reliable for activity prediction. Model IV and V produced a poor correlation of 0.897 and 0.844 with a cross-validated prediction RMSE of 0.627 and 0.622 using 11 and 12 compounds, with average analysis variance of 0.257 and 0.295, respectively. The prediction potential of model IV and V is very poor compared to the previous models. Based on the results of the final 3D-QSAR, model I was selected and was found to hold the best predictive potential. The maximal deviation of the superimposed biophoric centers and on the elimination of one or two compounds with large residuals, the statistics showed an improved correlation in certainn Apex-3D training set models. Elimination of compounds **9** and **11** in model I was further rationalized by analyzing the volumes.

Volumes. Apex-3D has aligned all the compounds in the biophore model, though they are different in biological activity. This is rationalized by examining the volume difference. Molecular volumes of the compounds used in the final Apex-3D analysis were visualized through Boolean grid representations of the superimposed compounds. The total volume of the 13 compounds and their volume difference with compound **9** and **11**, in which the pentoxy substituent in **9** and two phenyl rings in **11** protrudes from the union volume of a set of compounds, were calculated and are shown in Figures 6 and 7. The most significant difference volume is occupied by the pentoxy group in **9** and two phenyl rings in **11**. Both of these compounds are active still not considered by Apex-3D, hence these compounds must be interacting with auxiliary binding site of the receptor.

The electrostatic potential similarity calculation and optimization have been performed for the comparative evaluation of 13 cytochrome P-450$_{14\alpha DM}$ receptor ligands using the Hodgkin index as discussed by Good et al.[21] for multiple molecules. The electrostatic potential similarity between each pair of molecules as well as the overall similarity showed a good similarity, which is about 0.560. There is a slight improvement in electrostatic potential fitting of 0.565 when compounds **9** and **11** are not considered. Thus, both geometrical and electronic properties must be taken into consideration in order to rationalize their efficacy.

CONCLUSION

The Apex-3D methodology has been applied for 13 chemically diverse training sets of azole antifungal agents having binding affinity to cytochrome P-450$_{14\alpha DM}$. The resulting 3D-QSAR model derived from a training set of 11 compounds and the elimination of compounds **9** and **11** from the initial Apex-3D analysis show a significant correlation

of steric factors with biological activity. The predictions are very well in agreement with the experimental values. This rationalizes the binding affinity in terms of steric properties. The Apex-3D biophore model reveals regions in 3D space around these ligands and provides a hypothetical picture of the main structural features responsible for MIC variations. The Apex-3D biophore model generated in this study should be useful for the design of novel antifungal agents.

ACKNOWLEDGMENT

The authors thank the All India Council for Technical Education (AICTE), New Delhi and FDC, Ltd., Mumbai for the financial support.

REFERENCES AND NOTES

(1) Presented in part at the First Indo−U.S. Workshop on Mathematical Chemistry, Santiniketan, West Bengal, India, January 9−13, 1998.
(2) Tafi, A.; Anastassopoulou, J.; Theophanides, T.; Botta, M.; Corelli, F.; Massa, S.; Artico, M.; Costi, R.; Di Santo, R.; Ragno, R. Molecular Modeling of Azole Antifungal Agents Active Against *Candida albicans*. 1. A Comparative Molecular Field Analysis Study. *J. Med. Chem*. **1996**, *39*, 1227−1235.
(3) Hitchcock, C. A.; Dickinson, K.; Brown, S. B.; Evans, E. G. V.; Adams, D. J. Interaction of Azole Antifungal Antibiotics with Cytochrome P-450 Dependent 14 α-Sterol Demethylase Purified from *Candida albicans*. *Biochem. J*. **1990**, *266*, 475−480.
(4) Yoshida, Y.; Aoyama, Y. Interaction of Azole Antifungal Agents with Cytochrome P-$450_{14\alpha DM}$ Purified from *Saccharomyces cerevisiae* Microsomes. *Biochem. Pharmacol*. **1987**, *36*, 229−235.
(5) Goldman, R. C.; Klein, L. L. Problems and Progress in Opportunistic Infections. In *Annual Reports in Medicinal Chemistry*; Bristol, A. J.; Ed.; Academic Press: San Diego, CA, 1994; Vol. 29, pp 155−164.
(6) Odds, F. C.; Schmid, J.; Soll, D. R. Epidemiology of Candida infections in AIDS. In *Mycoses in AIDS Patients*; Vanden Bossche, H., Ed.; Plenum Press: New York, 1990; pp 67−74.
(7) Fromtling, R. A. *Drugs of the Future* **1985**, *10*, 983−984.
(8) Sammes, P. G. In *Topics in Antibiotic Chemistry*; Sammes, P. G., Ed.; Ellis Horwood Limited: Chichester, 1982; Vol. 6, Chapter 1, pp 22−97.
(9) *Drugs of the Future* **1981**, *6*, 444−445.
(10) *Drugs of the Future* **1988**, *13*, 624−626.
(11) Benfield, P.; Clissold, S. P. Sulconazole: A Review of its Antimicrobial Activity and Therapeutic use in Superficial Dermatomycoses. *Drugs* **1988**, *35*, 143−153.
(12) Xavier, R.; Hopkins, S. J. Neticonazole: A New and Highly active imidazole antifungal agent. *Drugs of Today* **1994**, *30*, 497−505.
(13) Plempel, M.; Regel, E.; Buchel, K. H. Antimycotic Efficacy of Bifonazole in Vitro and in Vivo. *Arzneim.-Forsch.* **1983**, *33*, 517−524.
(14) Bartoli, J.; Alguero, M.; Boncomte, E.; Forn, J. Synthesis and Antifungal Activity of a Series of Difluorotritylimidazoles. *Arzneim.-Forsch.* **1992**, *42*, 832−835.
(15) Michel, G. *Drugs of Today* **1993**, *29*, 307−310.
(16) Golender, V.; Vorpagel, E. In *3D QSAR in Drug Design: Theory, Methods and Applications*; Kubinyi, H., Ed.; ESCOM: Leiden, 1993; pp 137−149.
(17) Van de Waterbeemd, H. In *Advanced Computer-Assisted Techniques in Drug Discovery*; Van de Waterbeemd, H., Ed.; VCH Publishers: New York, 1994; Vol. 3.
(18) INSIGHT II (v. 95.0); Molecular Simulations Inc.: 9685 Scranton Road, San Diego, CA 92121-3752, U.S.A., October 1995.
(19) Molecular Simulations Inc., San Diego, CA.
(20) Talele, T. T.; Hariprasad, V.; Kulkarni, V. M. Docking Analysis of a Series of Cytochrome P-$450_{14\alpha DM}$ Inhibiting Azole Antifungals. *Drug Design Discovery* **1998**, *15*, 181−190.
(21) Good, A. C.; Hodgkin, E. E.; Richards, W. G. The utilization of Gaussian Functions for the Rapid Evaluation of Molecular Similarity. *J. Chem. Inf. Comput. Sci*. **1992**, *32*, 188−191.
(22) Hariprasad, V.; Kulkarni, V. M. A proposed common spatial pharmacophore and the corresponding active conformations of some peptide leukotriene receptor antagonists. *J. Comput.-Aided Mol. Design* **1996**, *10*, 284−292.
(23) Mottola, D. M.; Lauter, S.; Watts, V. J.; Tropsha, A.; Wyrick, S. D.; Nichols, D. E.; Mailman, R. B. Conformational Analysis of D_1 Dopamine Receptor Agonists: Pharmacophore Assessment and Receptor Mapping. *J. Med. Chem*. **1996**, *39*, 285−296.
(24) Myers, R. H. In *Classical and Modern Regression with Application*; PWS−KENT Publishing Company: 1990.
(25) Marshal, G. R.; Barry, C. D.; Bosshard, H. E.; Dammkoehler, R. A.; Dunn, D. A. The Conformational Parameter in Drug Design: the Active Analogue Approach. In *ACS Symp. Ser*. **1979**, *112*, 205−226.

CI9800413